Structural and Mechanistic Studies of Arylalkylhydrazine Inhibition of Human Monoamine Oxidases A and B[†,‡]

Claudia Binda,[§] Jin Wang,[||] Min Li,[⊥,||] Frantisek Hubalek,[#,||] Andrea Mattevi,[§] and Dale E. Edmondson*[,||]

Department of Genetics and Microbiology, University of Pavia, via Ferrata 1, Pavia 27100, Italy, and Departments of Biochemistry and Chemistry, Emory University, Atlanta, Georgia 30322

Received February 18, 2008; Revised Manuscript Received March 25, 2008

ABSTRACT: The structure and mechanism of human monoamine oxidase B (MAO B) inhibition by hydrazines are investigated and compared with data on human monoamine oxidase A (MAO A). The inhibition properties of phenylethylhydrazine, benzylhydrazine, and phenylhydrazine are compared for both enzymes. Benzylhydrazine is bound more tightly to MAO B than to MAO A, and phenylhydrazine is bound weakly by either enzyme. Phenylethylhydrazine stoichiometrically reduces the covalent FAD moieties of MAO A and of MAO B. Molecular oxygen is required for the inhibition reactions, and the level of O_2 consumption for phenylethylhydrazine is 6−7-fold higher with either MAO A or MAO B than for the corresponding reactions with benzylhydrazine or phenylhydrazine. Mass spectral analysis of either inhibited enzyme shows the major product is a single covalent addition of the hydrazine arylalkyl group, although lower levels of dialkylated species are detected. Absorption and mass spectral data of the inhibited enzymes show that the FAD is the major site of alkylation. The three-dimensional (2.3 Å) structures of phenylethylhydrazine- and benzylhydrazine-inhibited MAO B show that alkylation occurs at the N(5) position on the *re* face of the covalent flavin with loss of the hydrazyl nitrogens. A mechanistic scheme is proposed to account for these data, which involves enzyme-catalyzed conversion of the hydrazine to the diazene. From literature data on the reactivities of diazenes, O_2 then reacts with the bound diazene to form an alkyl radical, N_2 and superoxide anion. The bound arylalkyl radical reacts with the N(5) of the flavin, while the dissociated diazene reacts nonspecifically with the enzyme through arylalkylradicals.

Of the current six FDA-approved monoamine oxidase (MAO)[1] inhibitors, one of the original clinically used compounds is phenylethylhydrazine (phenelzine) (*1*). The original discovery of hydrazines as effective MAO inhibitors by Zeller (*2*) came from the observation that TB patients receiving isoniazid therapy experienced mood elevation, and thus, phenylethylhydrazine was developed for use as a MAO inhibitor (MAO-I) for the treatment of depression. Although still clinically available, the side effects of phenylethylhydrazine inhibition of MAO included hypertension resulting from the ingestion of foods that contain high levels of tyramine that later became well-known as the cheese effect. Early studies found that phenylethylhydrazine inhibition of MAO is irreversible and that both MAO A and MAO B are inhibited, suggesting little specificity for the action of the drug. Subsequent work reported that other arylalkylhydrazines such as phenylhydrazine and benzylhydrazine are also irreversible inhibitors of MAO (*3*).

The mode of irreversible MAO inhibition involves covalent modification of the flavin coenzyme since the visible absorption spectrum of hydrazine-inhibited MAO resembles that of a reduced flavin chromophore that is not reoxidized by exposure to molecular oxygen. Similar properties on inhibition are also shown by the bacterial amine oxidizing enzyme (trimethylamine dehydrogenase) (*4*). Nagy et al. (*4*) found that incubation of FMN with phenylhydrazine in the dark for a number of days led to the formation of an alkyl flavin with spectral properties of flavin hydroquinone, which they assigned to be a flavin C(4a) phenyl adduct on the basis of UV−vis absorption data, mass spectral, and infrared spectral data (Scheme 1). Kim et al. (*5*) demonstrated that phenylhydrazine or benzylhydrazine form 4a alkyl adducts with the model N(5)-ethyllumiflavinium perchlorate system. These results have led to the general assumption in the literature that MAO A or MAO B inhibition is a result of alkylation of the flavin (4a) position by the hydrazine with an apparent loss of molecular nitrogen from the hydrazyl moiety since no evidence is apparent that the hydrazine functionality remains intact on inhibition (*6*). The alkylation

[†] This work was supported by grants from the National Institute of General Medical Sciences (GM-29433), MIUR (COFIN06), and Regione Lombardia. The mass spectrometry equipment of the Emory University Microchemical Facility used throughout this work was purchased by National Institutes of Health shared Instrumentation Grants NCRR-02878, NCRR-12878, and NCRR-13948.

[‡] Atomic coordinates have been deposited in the Protein Data Bank with codes 2vrl and 2vrm.

* To whom correspondence should be addressed. Dr. Dale E. Edmondson. Department of Biochemistry, Emory University, 1510 Clifton Rd., Atlanta, GA 30322. Phone: 404-727-5972. Fax: 404-727-2738. E-mail: deedmon@emory.edu.

[§] University of Pavia.

[||] Emory University.

[⊥] Present address: Department of Biochemistry and Biophysics, University of California, San Francisco, CA 94107.

[#] Present address: Novo Nordisk A/S, DK0-2880 Bagsvaerd, Denmark.

[1] Abbreviations: MAO, monoamine oxidase; MAO-I, MAO inhibitors; MMTP, 1-methyl-4-(1-methyl-1*H*-pyrrol-2-yl)-1,2,3,6-tetrahydropyridine; ESR, electron spin resonance.

10.1021/bi8002814 CCC: $40.75
Published on Web 04/22/2008

Scheme 1: Proposed Structure of Flavin C(4a) Adduct formed on Reaction of FMN with Phenylhydrazine (from Nagy et al. (*4*))

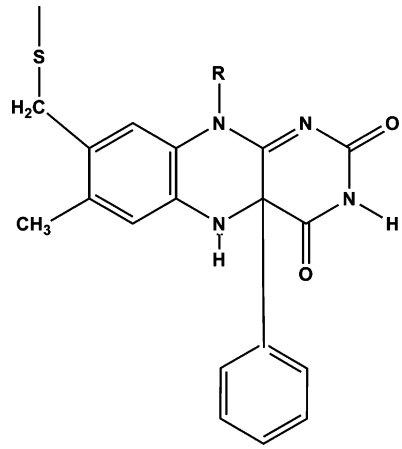

of a coenzyme by arylalkylhydrazines is markedly similar to the results from Ortiz de Montellano's laboratory who showed that phenylethylhydrazine inhibition of cytochrome P450 results in heme alkylation by an apparent radical mechanism (*7*). Fitzpatrick and Villafranca (*8*) demonstrated that benzylhydrazine inhibition of dopamine β-monooxygenase is a radical process with alkylation of an unknown amino acid residue presumably at the active site.

With the development of expression systems to provide human MAO B and MAO A in high yields (*9, 10*) and the determination of the crystal structures of both enzymes (*11, 12*), it was of interest to investigate in more detail the structures and mechanisms of MAO A and B inhibition by arylalkylhydrazines. Since hydrazines are known to undergo radical chemistry, this approach might also serve to further probe possible radical mechanisms in the active sites of these enzymes since the mechanism of amine oxidation in catalysis is still a controversial topic on whether catalysis occurs via an amininium cation radical mechanism (*13*), a hydride transfer reaction (*14, 15*), or a polar nucleophilic mechanism (*16*). The availability of pure human MAO A (*10*) and of pure human MAO B (*9*) allow comparative studies on the interaction of either enzyme with the arylalkylhydrazines and a more definitive molecular understanding of the specificity of phenelzine when administered to the human. These comparative studies are reported in this article as well as the three-dimensional structures of human MAO B after inhibition with phenylethylhydrazine and with benzylhydrazine. The results show that both enzymes are inhibited by similar mechanisms and that O_2 is required for inhibition but that differing affinities are exhibited from comparisons of data obtained with phenylethylhydrazine, benzylhydrazine, and phenylhydrazine. The structure of the inhibited forms of MAO B show irreversible alkylation to occur specifically at the flavin ring N(5) position.

MATERIALS AND METHODS

Materials. All amine substrates used in this study were either purchased from Sigma-Aldrich at the highest purity available (>98%) or synthesized and characterized as described previously (*17*). The arylalkylhydrazines including phenylethylhydrazine, *p*-bromophenylhydrazine, benzylhydrazine, and phenylhydrazine were purchased from Sigma-Aldrich and used without further purification. All hydrazine solutions and reaction solutions were prepared in buffers containing 1 mM EDTA to minimize trace metal catalyzed oxidation by atmospheric oxygen. The MAO substrate 1-methyl-4-(1-methyl-1*H*-pyrrol-2-yl)-1,2,3,6-tetrahydropyridine (MMTP) (*18*) was a generous gift from Dr. Neal Castignoli, Department of Chemistry, Virginia Tech University.

Expression and Purification of Human Monoamine Oxidases. Recombinant human liver MAO A and MAO B were expressed in the methylotrophic yeast *Pichia pastoris* and purified as described previously (*9, 10*).

Steady-State Enzyme Assays. Steady-state kinetic studies were performed spectrophotometrically using a Perkin-Elmer Lambda 2 UV−vis spectrophotometer. The oxygen concentration in all assays was at air saturation (~240 μM). MAO A kinetic assays were carried out in 50 mM potassium phosphate buffer (pH 7.5) containing 0.5% (w/v) reduced Triton X-100 following the oxidation of 1 mM kynuramine by the change in absorbance at 316 nm (product 4-hydroxyquinone absorbance, $\Delta\varepsilon = 12{,}000\ M^{-1}\ cm^{-1}$) (*19*) with time. One unit activity of MAO A is defined as the amount of enzyme that is able to catalyze the formation of 1 μmol of 4-hydroxyquinone per minute. MAO B kinetic assays were carried out in either 50 mM HEPES or phosphate buffers (pH 7.5) containing 0.5% (w/v) reduced Triton X-100. MAO B activity was determined following the oxidation of benzylamine (3 mM) from the change in absorbance at 250 nm (product benzylaldehyde absorbance, $\Delta\varepsilon = 11{,}800\ M^{-1}\ cm^{-1}$) with time. One unit activity of MAO B was defined as the amount of enzyme that is able to catalyze the formation of 1 μmol benzaldehyde per minute. All kinetic data were analyzed using Microcal Origin software on a PC. Activity data with MAO A using *p*-CF_3-benzylamine or MMTP gave results identical to those observed with kynuramine. Similarly, activity assays with MAO B using either kynuramine or MMTP as substrates gave results identical with those observed with benzylamine.

Oxygen Uptake Experiments. Oxygen uptake experiments were determined polarographically using an YSI model 53 oxygen electrode system with its output connected to a Nicolet 4094 digital oscilloscope. A fabricated 3 mL water-jacketed cell accommodated the electrode with continuous stirring. The changes in O_2 concentration in solution are then digitally recorded for subsequent analysis.

UV−Vis Spectroscopic Experiments. All UV−vis spectral studies of MAO A and MAO B were carried out on a Cary 50 UV−vis spectrophotometer. Anaerobic spectral experiments were carried out under an Ar atmosphere using a quartz cuvettes fabricated as described previously (*20*).

Analytical HPLC and Mass Spectral Analysis. The MAO A and MAO B samples were desalted prior to mass spectral measurements on intact protein using a microbore RP-HPLC consisting of a Model 140A solvent delivery system and a Model 1000S diode-array UV detector (PE-Biosystems, Foster City, CA). Electrospray ionization mass spectral measurements were performed using a Model API3000 triple quadrupole mass spectrometer (PE-Sciex, Foster City, CA) equipped with the MicroIonSpray electrospray source. MAO A and MAO B were inactivated with 10−100-fold molar excesses of hydrazine analogues at room temperature (MAO B) or on ice (MAO A). After inactivation, flavin peptides were prepared for analysis by the following procedure. The

enzyme (~2.5 nmol) was precipitated with 5% (w/v) trichloroacetic acid, the pellet washed with water, and resuspended in 0.1 M ammonium bicarbonate. Chymotrypsin (5 μg) and trypsin (5 μg) were added to the suspension, and the samples were digested in dark for 15 h at 37 °C. A C2 reversed-phase extraction column (Alltech) was equilibrated with 3 mL of aqueous methanol and 1 mL of 50 mM ammonium bicarbonate prior to sample introduction. The column was sequentially washed with 1 mL of 50 mM ammonium bicarbonate, 1 mL of HPLC-grade water, and 1 mL of 5% (v/v) aqueous methanol. The flavin peptide was eluted with 5% (v/v) aqueous methanol, concentrated in a Speedvac, and analyzed by ESI-MS using precursor ion scanning set to detect the mass of the phosphate ion (due to the pyrophosphate moiety) in the FAD-containing peptide.

X-ray Crystallography. Purified human MAO B was incubated for 3 h with 2 mM inhibitor (either benzylhydrazine or phenyethylhydrazine) in the presence of 1 mM EDTA and complete bleaching of the protein sample was followed by UV−vis spectroscopy. Crystallization experiments were performed following published protocols (*21*), and colorless crystals grew in one week. X-ray diffraction data were collected at the beam-lines ID14-EH1 and ID14-EH2 of European Synchrotron Radiation Facility in Grenoble. For data collection, crystals were transferred into a mother liquor solution containing 2 mM inhibitor, 18% (v/v) glycerol, and flash-cooled in a stream of gaseous nitrogen at 100 K. Data processing and scaling (Table 4) were performed using MOSFLM (*22*) and programs of the CCP4 package (*23*). The structure of MAO B in complex with isatin (*21*) after removal of all water and inhibitor atoms was used as initial model and unbiased $2Fo - Fc$ and $Fo - Fc$ maps allowed to unambiguously model the inhibitors (Figure 6). Crystallographic refinements (Table 5) were performed with Refmac5 (*24*) and WARP (*25*), manual rebuilding was done with Coot (*26*). Tight noncrystallographic symmetry restraints were applied throughout the refinement calculations. Structural figures were produced by using Bobscript (*27*) and Raster3d (*28*).

RESULTS

Rates and Binding Parameters for MAO A and MAO B Inhibition. Incubation of purified preparations of human MAO A or MAO B with the hydrazines used in this work (phenylethylhydrazine, benzylhydrazine, or phenylhydrazine) result in the irreversible inhibition of either enzyme. Previous studies by Yu and Tipton (*29*) have shown that phenylethylhydrazine functions as a competitive inhibitor for benzylamine oxidation by rat liver mitochondrial MAO. Indeed, phenylethylhydrazine also functions as a competitive inhibitor for human MAO A and for human MAO B with K_i values in the micromolar region (Table 1). Benzylhydrazine also is a reasonable competitive inhibitor ($K_i = 26$ μM) for MAO B but a very poor inhibitor ($K_i \sim 2$ mM) of MAO A. Phenylhydrazine is bound poorly by either MAO A or by MAO B as judged by the hydrazine concentration required to observe competitive inhibition for either enzyme.

To further investigate the relative interactions of these arylalkylhydrazines with MAO A and MAO B, the concentration dependencies for the rates of inactivation of the enzymes were determined and analyzed by Kitz−Wilson plots (*30*) of the data (Table 1). Phenylethylhydrazine is bound to and inactivates MAO A approximately 6-fold more strongly than MAO B as judged from relative values of k_{inact}/K_{inact} values. It is of interest that the level of MAO B inactivation by phenylethylhydrazine approached 50% even at a 1 mM concentration, whereas MAO A is completely inhibited at concentrations ~200 μM. Benzylhydrazine interacts with MAO B 16-fold more strongly than with MAO A, and either enzyme is completely inhibited by benzylhydrazine at concentrations ~150 μM. Phenylhydrazine interacts with MAO A with a slightly higher affinity (~2-fold) than with MAO B. Phenylhydrazine completely inactivates MAO B at a concentration of 350 μM while MAO A requires concentrations ~1 mM for complete inhibition.

It is of interest to compare the relative values of K_i with that of K_{inact} shown in Table 1. There is reasonable agreement given that K_i values were determined at 25 °C, while K_{inact} data were determined at 15 °C. The reason for the lower temperature used in the inactivation experiments is due to the instability of purified human MAO A to incubation at 25 °C, while it is stable at 15 °C over the time span required for the experiments (*16*). The largest deviation in values occurs with MAO B with phenylethylhydrazine (~8-fold). These data suggest that K_{inact} is not a simple binding constant for phenylethylhydrazine binding to MAO B but that other reversible steps are required in the inactivation process. The reason these steps are not apparent with the other examples may result from the magnitudes of relative rate constants. It is known from the work in Tipton's (*29*) and in Hellerman's laboratories (*3*) that MAO catalyzes the oxidation of phenylethylhydrazine to form the hydrazone as well as the diazene and therefore the enzyme catalyzed oxidation of hydrazines can be viewed as mechanism-based inhibition.

Stoichiometries of MAO Interaction with Hydrazine Analogues. Since phenylethylhydrazine functions as the best MAO A inhibitor, it was of interest to probe the stoichiometry of enzyme bound flavin reduction and whether inactivation occurred under anaerobic conditions. The data in Figure 1 show spectral changes resulting from an anaerobic titration of MAO A with phenylethylhydrazine. The spectral changes are consistent with the 2-electron reduction of the enzyme bound flavin to its hydroquinone form without any observable intermediate stable semiquinone formation. A plot of the changes in absorbance with molar ratio of the hydrazine to enzyme ratio demonstrates a 1:1 molar stoichiometry for the process. Removal of an aliquot of enzyme under anaerobic conditions and assaying the enzyme shows >95% retention of catalytic activity after the titration (which required over an hour to complete). These results demonstrate the requirement for O_2 in the inactivation process, which is consistent with enzyme-catalyzed turnover as a component of the inactivation process. Similar results are observed in parallel experiments performed with MAO B (data not shown).

To further investigate this process, the stoichiometry of O_2 uptake was determined for the inactivation of MAO A and for MAO B with each of the hydrazines under investigation. The data in Figures 2 and 3 show that the addition of an arylalkylhydrazine to a solution of MAO A or of MAO B results in the consumption of O_2 to a level dependent on the concentration of enzyme and differed with the identity of hydrazine used. The level of O_2 consumed before the reaction ceases arises either from the reduction of the O_2

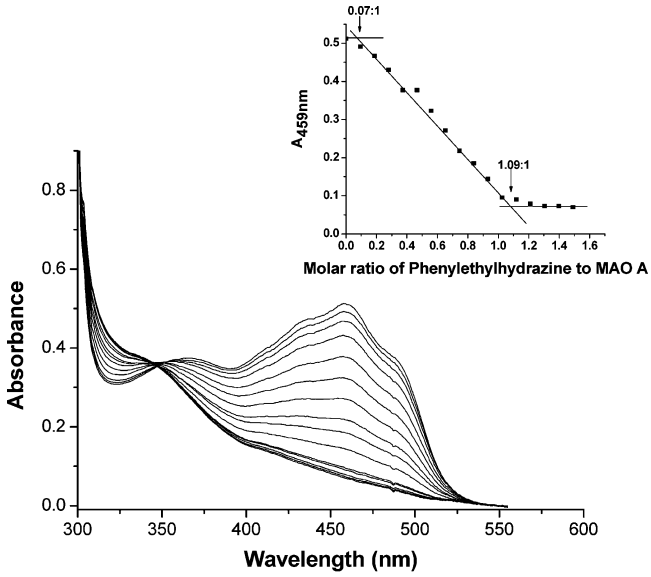

FIGURE 1: UV−vis absorption spectra of purified recombinant human liver MAO A (40 μM) in 50 mM potassium phosphate buffer at pH 7.5 with 0.5% (w/v) reduced Triton X-100 after a series of anaerobic addition of phenylethylhydrazine solution. Each spectral trace is after the addition of 10 μL of anaerobic hydrazine solution (400 μM). EDTA (1 mM) is included in both the enzyme and inhibitor buffers. The inset shows the plot of absorbance changes at $A_{459\ nm}$ as a function of the molar ratio of hydrazine to enzyme FAD.

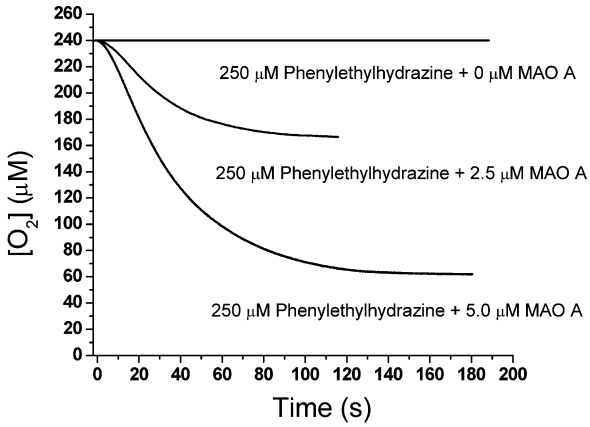

FIGURE 2: Effect of MAO A concentration on the level of O_2 consumption in the presence of 250 μM phenylethylhydrazine in 50 mM potassium phosphate, 1 mM EDTA, and 0.5% (w/v) reduced Triton X-100 at 25 °C.

concentration by catalytic turnover or from inhibition of enzyme activity.

For either MAO A or for MAO B, a stoichiometry of ~36−40 mol of O_2 per mol of enzyme-FAD (E-FAD) is required before the reaction ceases. After an initial brief lag phase (the observed lag phase is a result of the response time of the electrode), the rate of O_2 uptake follows a pseudo first-order kinetic behavior, which could be fit with a limiting rate constant of 1.7 min^{-1} (rates determined at differing phenylethylhydrazine concentrations with a constant [O_2] of 240 μM); a rate approximately double that of the limiting rate of inactivation. The rate of O_2 consumption for benzylhydrazine incubation with MAO A is estimated to be ~1 min^{-1} and that for phenylhydrazine (at 5 mM concentration) is 0.09 min^{-1} (Table 2). The low binding affinities of MAO A for either benzylhydrazine or for phenylhydrazine precluded definitive determinations of the respective limiting

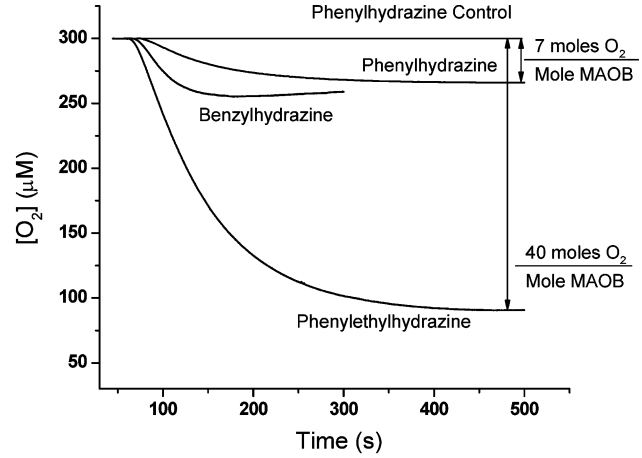

FIGURE 3: Comparisons of rates and extents of O_2 consumption on the addition of 500 μM phenylhydrazine, 500 μM benzylhydrazine, or 500 μM phenylethylhydrazine (final concentrations) to solutions of 5 μM MAO B in 50 mM potassium phosphate, 1 mM EDTA, and 0.5% (w/v) reduced Triton X-100 at 25 °C.

Table 1: Comparison of MAO A and MAO B K_i Values and Limiting Rates of Inactivation and K Inactivation with Selected Arylalkylhydrazines

	K_i (μM)[a]	K_{inact} (μM)[b]	k_{inact} (min^{-1})[b]	k_{inact}/K_{inact} (M^{-1}-min^{-1})
		phenylethylhydrazine		
MAO A	47 ± 2	50 ± 1	0.90 ± 0.01	18
MAO B	15 ± 2	128 ± 2	0.43 ± 0.03	3
		benzylhydrazine		
MAO A	2096 ± 258	1950 ± 60	3.1 ± 0.1	1.6
MAO B	26 ± 1	48.4 ± 2.4	1.28 ± 0.03	26
		phenylhydrazine		
MAO A	205 ± 4	523 ± 64	0.10 ± 0.01	0.2
MAO B	ND[c]	791 ± 135	0.34 ± 0.05	0.4

[a] Determined from competitive inhibition data of substrate oxidation at 25 °C. [b] Determined from Kitz−Wilson plots of the hydrazine concentration dependence on rates in enzyme inhibition at 15 °C. [c] No detectable competitive inhibition was observed up to a hydrazine concentration of 100 μM.

Table 2: Comparison of Stoichiometries and Rates of O_2 Consumption on MAO Inactivation

	moles O_2 consumed/ mol E-FAD	rate of O_2 uptake during inactivation (min^{-1})
	phenylethylhydrazine	
MAO A	35−40	1.7
MAO B	35−40	1.4
	benzylhydrazine	
MAO A	8	1.0
MAO B	6	1.7
	phenylhydrazine	
MAO A	7	0.1
MAO B	7	0.7

rates for these hydrazines. In both cases, the rates of O_2 uptake were similar to the respective rates of k_{inact} (Table 1). The stoichiometries of O_2 uptake for benzylhydrazine (8 moles O_2/ mole E-FAD and phenylhydrazine (7 mol O_2/mol E-FAD) are considerably lower for MAO A or MAO B (Table 2) than is observed with phenylethylhydrazine. These data demonstrate that phenylethylhydrazine interaction with MAO A or MAO B undergoes a considerable number of catalytic turnovers before enzyme inactivation. In the case

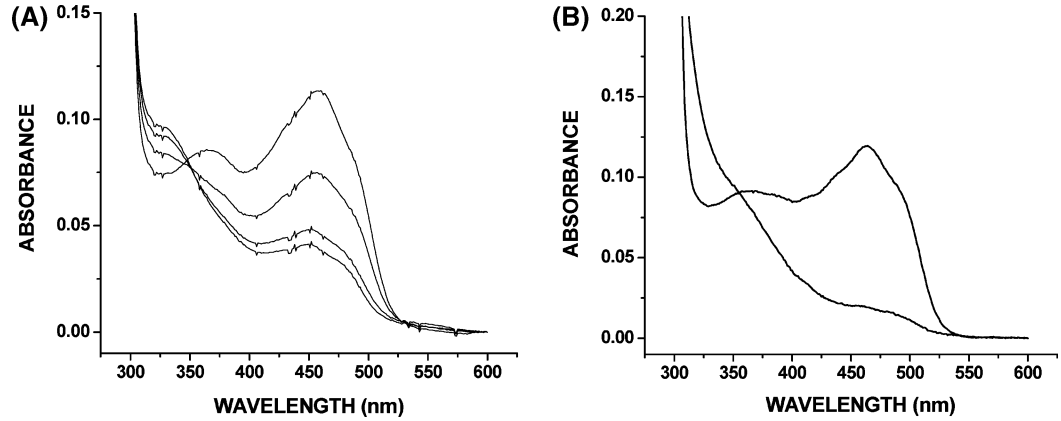

FIGURE 4: Absorption spectra of MAO A (including intermediate spectra during the inhibition reaction) (A) and MAO B (B) after inhibition with phenylethylhydrazine. The enzymes are dissolved in 50 mM potassium phosphate at pH 7.5 containing 0.5% (w/v) reduced Triton X-100.

of benzylhydrazine or phenylhydrazine, the ratio of catalytic turnovers to inactivation events is considerably smaller.

The stoichiometries of O_2 consumption for MAO B closely parallel the results obtained for MAO A. A molar stoichiometry of >90 mol of O_2 are consumed before the enzyme is inactivated by phenylethylhydrazine (Table 2) and 6 and 7 mol, respectively, for benzylhydrazine and phenylhydrazine inactivation. The relative estimated rate constants for O_2 uptake for the three hydrazine analogues are slightly faster than the observed k_{inact} rates shown in Table 1 and faster than those observed for MAO A (Table 2).

Visible Absorption Spectral Changes in MAO A and in MAO B on Hydrazine Inhibition. Previous studies published from the Hellerman (*3*) and Singer (*4*) laboratories showed that hydrazine inhibition of bovine MAO B resulted in irreversible spectral changes in the flavin absorption region of the spectrum, which has been attributed to alkylation of the C(4a) position of the flavin ring (Scheme 1) (*4*). The spectral data in Figure 4B show that MAO B inactivation by phenylethylhydrazine results in alterations of the enzyme bound flavin as the spectral change in which the flavin 450 nm region is nearly completely bleached to resemble that of an alkylated flavin. Similar experiments with MAO A (Figure 4A) result in essentially identical spectral data leading to inhibited enzyme samples exhibiting spectral characteristics of covalently modified flavins since no return of the oxidized spectra or catalytic activities are observed on dialysis or gel filtration of the inhibited enzymes.

Mass Spectral Analysis of Hydrazine-Inhibited MAO A and MAO B. Previous results from Hellerman's laboratory (*3*) and from Singer's laboratory (*4*) using ^{14}C labeled phenylhydrazine with bovine MAO B suggested a stoichiometry higher than 1:1 for covalent binding to the enzyme. Patek and Hellerman (*3*) measured a stoichiometry of 1.4 mol of phenyl ring/mol of enzyme subunit, which has been also observed by Kenney et al. for bovine liver MAO B (*6*). One explanation for this apparent stoichiometry is the lability of phenylhydrazines in aerobic aqueous solutions and the relatively high concentrations required for MAO B inhibition (see Table 1). Previous results from this laboratory have demonstrated that the high resolution mass spectrometry of MAO A or of MAO B can readily resolve differences in molecular weight due to the incorporation of small molecular weight molecules as small as *N*-ethymaleimide modification

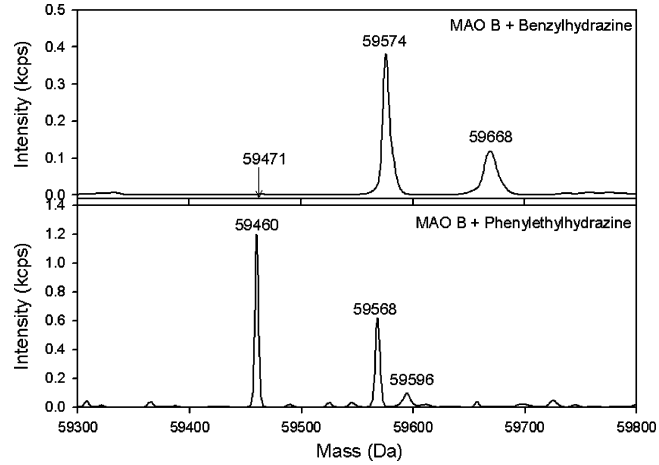

FIGURE 5: Electrospray mass spectrum of MAO B after inhibition by benzylhydrazine and by phenylethylhydrazine. The mass at 59,475 Da is that of the unmodified enzyme, 59, 574 Da is MAO B with one arylalkyl group from benzylhydrazine, and 59,668 Da is that of MAO B containing two arylalkyl groups of benzylhydrazine. The level of multialkylation is much lower for the phenylethylhydrazine-treated sample.

of thiol groups (*31*). Therefore, to monitor the stoichiometries of hydrazine analogue covalent modification of MAO A or MAO B, the inhibited enzymes were analyzed by high resolution mass spectrometry. The representative data are shown in Figure 5 and summarized in Table 3. The mass of purified MAO B (59,475 ± 8 Da) increases on inhibition with benzylhydrazine to a mass of 59,574 ± 28 Da). These data show an increased mass of 99 ± 10 Da as compared to an expected increase of mass of 91 Da if only the arylalkyl portion of benzylhydrazine is covalently incorporated. Another species (of lower amount) with a mass of 59,668 is probably due to the incorporation of a second benzyl species. Mass spectral results with phenylethylhydrazine inhibited MAO B show an increase in mass from 59,475 ± 14 Da to a mass of 59,568 ± 10 Da on inhibition with little or no detectable levels of multialkylated enzyme species (Figure 5). Minor levels of higher mass species are observed with phenylhydrazine inactivated samples (data not shown), which suggests some nonenzymatic modification of the enzymes resulting from the instability of high concentrations of phenylhydrazine in aerobic aqueous solutions and probably accounts for the >1.0 stoichiometries observed in previous studies (*3, 5*).

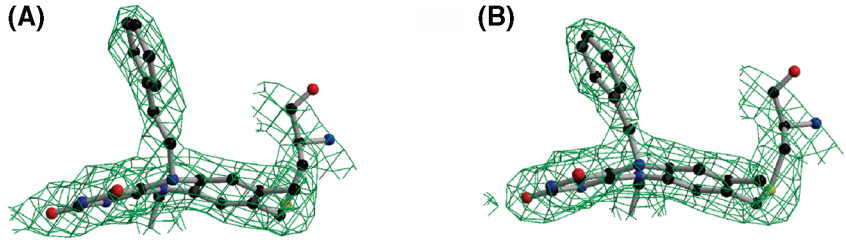

FIGURE 6: Structures of MAO B flavin adducts formed after inhibition with phenylethylhydrazine (A) and after inhibition with benzylhydrazine (B).

Table 3: Electrospray Mass Spectrometry of MAO A and MAO B after Inhibition by Selected Arylalkylhydrazines

	observed mass (Da)	calculated mass (Da)[a]	difference (da)
MAO A	60,518 ± 8	60,510	2
phenyhydrazine	60,617 ± 35	60,587	30
benzylhydrazine	60,599 ± 12	60,601	−2
phenylethylhydrazine	60,611 ± 10	60,615	−4
MAO B	59,475 ± 14	59,458	17
phenylhydrazine	59,551 ± 23	59,535	16
benzylhydrazine	59,576 ± 28	59,549	27
phenylethylhydrazine	59,568 ± 10	59,563	5

[a] Calculated mass included the enzyme sequence, N-terminal acetylation, the covalent FAD moiety, and the incorporation of a single arylalkyl moiety from the respective hydrazine used in the experiment.

Table 4: Mass Spectroscopic Mass Determinations of MAO A and MAO B Flavin Pentapeptides after Arylalkylhydrazine Inhibition[a]

	observed mass major peak (minor peak)	calculated mass thioether (sulfone)
no inhibition	1269.0	1269.0 (1285.0)
	MAO A	
phenylethylhydrazine	1391.4	1374.4 (1390.4)
phenylhydrazine	not detected	1347.2 (1363.2)
p-Br-phenylhydrazine[b]	1425.1 (1442.1)	1425.0 (1441.8)
	1427.1 (1444.1)	1426.8 (1443.5)
	MAO B	
phenylethylhydrazine	1391.4 (1374.9)	1374.4 (1390.4)
phenylhydrazine	1346.8 (1363.1)	1347.2 (1363.2)
p-Br-phenylhydrazine[b]	1425.2 (1442.1).	1425.0 (1441.8)
	1427.1 (1444.1)	1426.8 (1443.5)

[a] All masses determined using Precursor Ion Phosphate monitoring of tryptic/Chymotrytic FAD pentapeptides before and after enzyme inhibition with the indicated hydrazine analogue. [b] The two masses indicated are for the two natural isotopic abundance masses of the para-bromo substituent which serves as an internal control for the intactness of the arylalkyl moiety of the hydrazine analogue.

Mass spectral studies were also employed to define the probable site of alkylation as the covalent flavin moiety of the enzyme. Using precursor ion scanning MS/MS on tryptic/chymotryptic digests of purified inactivated enzymes, a higher level of mass resolution is achieved to verify the mass increase due to the covalent alkylating species. Precursor ion scanning MS (monitoring peptide masses by detection of phosphate mass) allows for the specific detection of the FAD peptide species in the presence of other peptides by its phosphate content since no other phosphate groups are found in the purified enzymes. The results in Table 4 show that, for both MAO A and MAO B, the site of alkylation is the flavin peptide and that the alkylating species is the arylalkyl group of the respective hydrazine analogue. Therefore, in all cases, the nitrogenous hydrazine moiety is released, leaving only the alkyl group. Of interest is the finding that the thioether linked flavin peptide is susceptible to oxidation to the sulfoxide as indicated by a mixture of thioether and thioether + 16 mass units resulting from the incorporation of 1 oxygen atom. In the case of the phenylethylhydrazine flavin peptide, the major peak observed is at the sulfoxide oxidation level. Since no precautions are taken to exclude O_2 from the enzyme on proteolytic digestion and peptide preparation, the oxidation of the labile thioether moiety to the sulfoxide is not surprising.

The phenylhydrazine flavin adduct of the MAO A flavin peptide was not detectable for unknown reasons, although it is observable with the MAO B sample. As an alternative, a *p*-bromophenylhydrazine inhibited sample was analyzed to serve as an internal control for the intactness of the aryl ring since the two natural isotopes of Br (79 and 81; each with approximately 50% abundance) would be observed if the intact arylalkyl group is the substituent on the flavin (Table 3).

X-ray Structural Studies of Inhibited MAO B. The mass spectral studies on both intact proteins and on the respective flavin peptides of MAOA and MAO B demonstrate that inhibition of either enzyme occurs by a single covalent modification of the flavin coenzyme by the alkyl group of the hydrazine. These data, however, do not answer the question as to what site on the flavin ring is modified or other structural details associated with enzyme inhibition.

Table 5: Crystallographic Data Collection and Refinement Statistics for Inhibited MAO B Crystals

	benzylhydrazine	phenylethylhydrazine
space group	*C*222	*C*222
unit cell (Å)	$a = 132.4$	$a = 130.9$
	$b = 223.9$	$b = 222.9$
	$c = 87.3$	$c = 86.4$
resolution (Å)	2.4	2.3
R_{sym}[a,b] (%)	8.5 (11.6)	11.3 (45.4)
completeness[b] (%)	92.1 (85.4)	98.3 (99.8)
unique reflections	46,894	55,095
redundancy	5.3	3.6
I/σ[b]	16.4 (5.0)	11.8 (2.8)
no. of atoms. protein/ligand/water	8017/2 × 7/289	8017/2 × 8/438
average *B* value for ligand atoms (Å^2)	21.0	21.9
R_{cryst}[c] (%)	18.7	20.0
R_{free}[c] (%)	23.4	24.6
rms bond length (Å)	0.012	0.012
rms bond angles (°)	1.29	1.28

[a] $R_{sym} = \Sigma|I_i - \langle I\rangle|/\Sigma I_i$, where I_i is the intensity of i^{th} observation, and $\langle I\rangle$ is the mean intensity of the reflection. [b] Values in parentheses are for reflections in the highest resolution shell. [c] $R_{cryst} = \Sigma|F_{obs} - F_{calc}|/\Sigma|F_{obs}|$ where F_{obs} and F_{calc} are the observed and calculated structure factor amplitudes, respectively. R_{cryst} and R_{free} were calculated using the working and test sets, respectively.

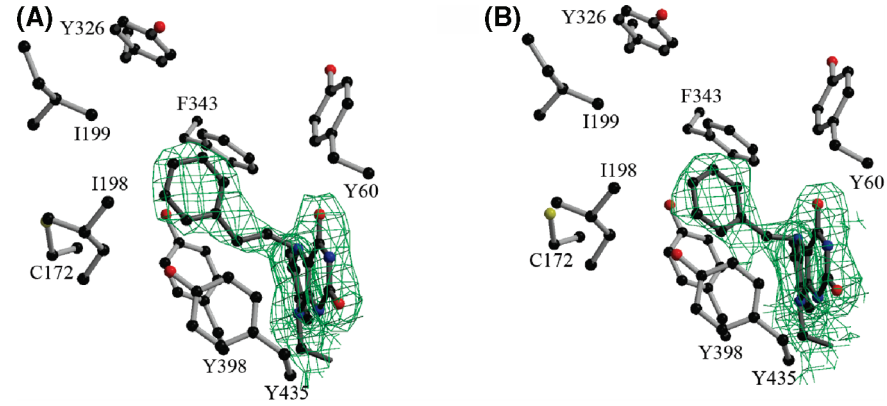

FIGURE 7: Structures of the active site amino acids about the phenylethyl N(5) adduct of MAO B (A) and the benzyl N(5) adduct of MAO B (B).

Since MAO B is more amenable to crystallization and the crystals diffract to a higher resolution (*21*) than that observed for MAO A (*12*), enzyme samples inhibited with phenylethylhydrazine and with benzylhydrazine were subjected to crystallization and their respective structures determined to 2.3 Å resolution. Attempts were made to determine the structure of phenylhydrazine inhibited MAO B, however, no clear electron density of the bound inhibitor could be observed. We do not have an explanation for these observations, although they may reflect incomplete binding or low occupancy. The determined structures show only a single covalent modification of the enzyme with either hydrazine analogue. Analysis of the structure of the modified covalent flavin moiety of MAO B shows that the flavin N(5) position is the site for flavin alkylation with either phenylethylhydrazine or with benzylhydrazine (Figure 6 A and B). In both structures, the modification occurs at the *re* face of the flavin ring, and the tricyclic ring is in a bent conformation (~30° from planarity) as observed in all other MAO B structures (*24*). The structural data clearly demonstrate that the nitrogenous hydrazine moieties are absent and that inactivation involves elimination of the nitrogens for either analogue.

The structures in Figure 7 show the interactions of the phenyl rings of the N(5) alkyl groups with amino acid residues in the active site of MAO B. In both structures, the phenyl ring of the adduct is in a perpendicular conformation to the flavin ring and have parallel π-interactions with Tyr398 and Tyr435, which constitute the aromatic cage in front of the flavin ring (*32, 33*). In both structures, the conformation of the Ile199 gate separating the entrance cavity from the substrate cavity (*34*) is in an open conformation (Figure 7).

DISCUSSION

Inhibition Requires Catalytic Turnover. The data presented here provide additional confirmation that phenylethylhydrazine functions as substrate for either MAO A or for MAO B and that benzylhydrazine functions as a substrate for MAO B. Evidence to support this conclusion is the reduction of either enzyme by 1 mol of hydrazine/mol of E-FAD under anaerobic conditions without detectable inactivation. These results are in agreement with previous studies by Yu and Tipton (*29*) who found that incubation of rat MAO with phenylethylhydrazine resulted in the formation of phenylacetaldehyde, which is derived from hydrolysis of the hydrazone product of enzyme oxidation. 2′-Deuteration of the phenylethyl side chain results in measurable kinetic isotope effects ($^{D}V\sim3$) demonstrating C−H bond cleavage in the reaction catalyzed. The potentiation of enzyme inhibition by 2′-deuteration of phenylethylhydrazine suggests that N−H bond cleavage to form the diazene is involved in the inhibition reaction, and 2′C−H bond cleavage is a turnover reaction in competition to the inhibition reaction (Scheme 2). The stoichiometries of O_2 uptake show that benzylhydrazine and phenylhydrazine exhibit fewer catalytic turnovers per inactivation event than does phenylethylhydrazine. The data presented here also support the view that enzyme catalyzed N−H bond cleavage occurs with all three hydrazines (with either MAO A or MAO B) to form their respective diazenes, which are involved in the inhibition reaction. The bond dissociation energy of the hydrazine N−H bond is similar to that of a benzyl C−H bond (*35*), and thus, MAO A or MAO B can cleave either moiety.

Enzyme Alkylation Leading to Irreversible Inhibition. Mass spectral data on either MAO A or on MAO B inactivated with phenylethylhydrazine and with phenylhydrazine demonstrate that the majority of enzyme is alkylated in a 1:1 stoichiometry. Smaller levels of enzyme with additional alkyl groups are observed, although the levels are much lower than the singly alkylated enzyme and difficult to quantify by mass spectrometry. Mass spectral analysis of the flavin peptides show that the flavin is monoalkylated with all hydrazines tested with either MAO A or MAO B. The mixture of flavin peptide peaks differing in mass by 16 is most likely due to the oxidation of the 8α-thioether linkage to the sulfoxide since the peptide is exposed to oxygen during denaturation and proteolyzis. Previous experience in this laboratory with 8α-*S*-cysteinyl flavins and flavin peptides has shown them to be readily oxidized to the 8α-sulfoxides under conditions required for proteolytic digestion of the enzymes. While the mass spectral data definitively demonstrate flavin alkylation by a single alkyl group of the hydrazine, these data do not allow assignment of the site of alkylation of the flavin ring and the testing of the proposal of Nagy et al. (*4*) that hydrazine alkylation of the flavin occurs at the C(4a) position of the flavin ring. It is well-known from the work of Walker et al. (*36*) that model N(5) alkyl flavins can isomerize to the more stable C(4a) alkylflavins. Such isomerization might occur during the time and conditions required for proteolysis of the alkyl flavin peptide for mass spectral analysis. The X-ray structural data on MAO B inactivated either with

Scheme 2: Reaction Schemes for MAO A or MAO B Oxidation of and Inhibition by Phenylethylhydrazine[a]

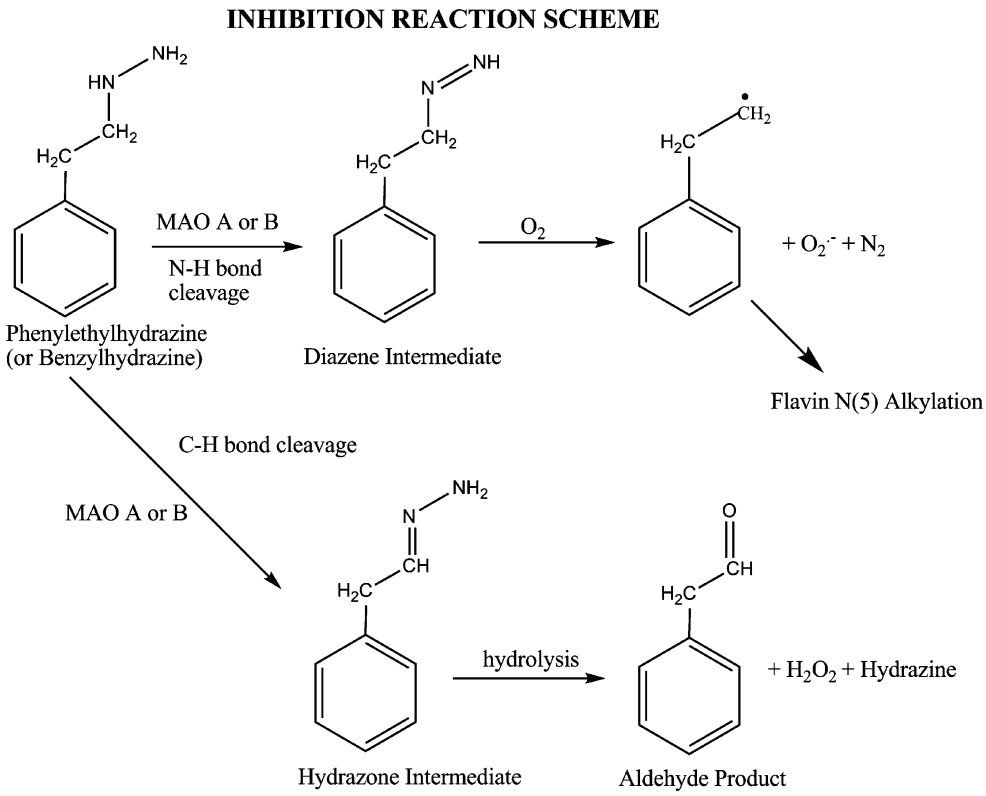

[a] The top scheme denotes the inactivation reaction, and the bottom scheme denotes the pathway for catalytic turnover.

phenylethylhydrazine or with benzylhydrazine demonstrate unequivocally that the site of flavin alkylation on the enzyme is at the N(5) position. The assignment by Nagy et al. (*4*) for a flavin C(4a) adduct on long-term incubation of FMN with phenylhydrazine probably is the result of the isomerization reaction discussed above (*36*). The structural data also show that the hydrazine nitrogens are lost during the inactivation event, thereby leaving a reactive alkyl group available for flavin modification. As observed with other MAO B irreversible inhibitors that react with the flavin N(5) position (*32*), the flavin ring conformation remains in its (~30°) bent state, identical with the conformation in oxidized enzyme crystallized with noncovalent inhibitors. Given the similar reactivity and mass spectral data on the reaction of MAO A with these hydrazines, we also conclude that the flavin site for alkylation in MAO A is also at the N(5) position.

Possible Mechanism of Inhibition. The data in this article as well as in a number of other earlier studies of hydrazine inhibition of MAO are consistent with the view that the initial step in the inactivation mechanism is the enzyme catalyzed cleavage of the hydrazine N−H bond to form the diazene (Scheme 2). This reaction results in the formation of the 2e-reduced flavin enzyme in complex with the diazene. Oxygen then reacts with the reduced enzyme to form H_2O_2 and oxidized flavin. A number of studies have shown that diazenes are very reactive entities and that they react very rapidly with oxygen to form superoxide anion, N_2, and the alkyl radical (*37, 38*). Alkyl radicals are very reactive with amino acid side chains (*39*), and therefore, one might expect to observe alkylated sites on the enzyme in addition to the flavin in the event that the diazene product dissociates from the enzyme to some degree prior to its reaction with O_2. This might account for the low levels of multiple alkylated enzyme species observed in the mass spectra of intact hydrazine inhibited enzyme. ESR spin trapping experiments using conditions as described previously (*7*) were performed to determine if there was any formation of alkyl radicals or oxygen radicals in solution during hydrazine inactivation of either MAO A or MAO B. Only trace levels of alkyl radicals were observed with signal intensities identical to that exhibited by control solutions of hydrazines in the absence of enzymes. The diffraction data on inhibited MAO B crystals showed no evidence for any alkylation sites other than the flavin. Therefore, if any diazene is released from the active site, it is probably at too low a level to be readily detectable.

We propose that the diazene formed as a result of the MAO catalyzed oxidation of the hydrazine moiety remains in the catalytic site and reacts with O_2 to form N_2, O_2^-, and the arylalkyl radical. Once formed, the alkyl radical could readily react with the flavin N(5) to form an N(5) alkylated species, which should be in its radical form with spectral properties of a neutral flavin semiquinone. No spectral evidence has been found for the formation of such a species, and therefore, an electron donor (possibly the O_2^-) could donate an electron to form the diamagnetic N(5) alkyl flavin. The fact that 6−8 mol of O_2 are required for each inactivation event with benzyl or phenylhydrazine suggests that at least 4−5 catalytic turnovers occur before enzyme alkylation occurs. The efficiency of enzyme inactivation relative to catalytic turnover is expected to be determined by the ratio of the rate of diazene release from the active site to its rate of reaction with O_2 while bound. Given that MAO A and

MAO B exhibit similar stoichiometries of O_2 consumption per inactivation event, these relative rates must be quite similar for the two enzymes. Preliminary experiments using the Y435F mutant of MAO B (*33*) show an O_2 stoichiometry of ~8 with phenylethylhydrazine rather than the value of ~40 observed with WT enzyme. The lower activity of this MAO B mutant (*33*) is consistent with the above discussion and is consistent with the finding that slowing catalysis by deuteration potentiates the rate of inactivation (*29*).

Relevance to Proposed Mechanisms of MAO Catalysis. It is of interest to note that biological hydrazine inhibition is observed most frequently with hemoproteins and metalloproteins such as Cu-dependent dopamine β-monooxygenase (*8*) or ribonucleotide reductase (*40*). Hydrazines are also well-known inhibitors of the quinoproteins by forming hydrazones with the carbonyl moieties of these TPQ-type cofactors (*41*). It is therefore of interest to ask the question as to how many flavoenzymes are irreversibly inhibited by the hydrazine class of compounds. On review of the literature, only the amine oxidases and amine dehydrogenases appear to be susceptible to hydrazine inhibition (at least by formation of an alkyl flavin adduct). No information has been published as to whether flavoenzymes such as D-amino acid oxidase are inhibited when exposed to compounds containing a hydrazine moiety. This situation may reflect the current view that the amino acid oxidases function by a hydride transfer mechanism (*14, 15*) and that there is no chemical precedent for a hydride abstraction from a hydrazyl moiety. The hydrazine hydrogens are acidic and proton abstraction would be the preferred mechanism for hydrogen removal. In the case of metalloenzymes, radical chemistry for hydrazine oxidation has been shown (*15*) as the Em value for 1-electron oxidation of hydrazines in the range of +250 to +500 mV (*40*). In the case of MAO, the measured 1-electron potentials for the flavin center is ~+40 mV (*42*) and therefore not a strong enough oxidant for the 1-electron oxidation of the hydrazine. The nucleophilicity of the terminal hydrazine N is greater than that of an amine due to the α-effect (*43*), and therefore, the most reasonable explanation for amine oxidase oxidation of hydrazines to their diazene forms is via a polar nucleophilic mechanism proposed previously (*16*) and recently reviewed (*44*). Further work is required to determine the detailed molecular mechanism of MAO catalyzed hydrazine oxidation and flavin adduct formation. This work provides a molecular framework for the design of detailed mechanistic approaches to define these reactions.

ACKNOWLEDGMENT

Ms. M. Aldeco provided excellent technical assistance during this project.

REFERENCES

1. Krishnan, K. R. (2007) Revisiting monoamine oxidase inhibitors. *J. Clin. Psychiatry 68*, 35–41.
2. Zeller, E. A., and Barsky, J. (1952) In vivo inhibition of liver and brain monoamine oxidase by 1-isonicotinyl-2-isopropyl hydrazine. *Proc. Soc. Exp. Biol. Med. 81*, 459–461.
3. Patek, D. R., and Hellerman, L. (1974) Mitochondrial monoamine oxidase. Mechanism of inhibition by phenylhydrazine and by aralkylhydrazines. Role of enzymatic oxidation. *J. Biol. Chem. 249*, 2373–2380.
4. Nagy, J., Kenney, W. C., and Singer, T. P. (1979) Reaction of Phenylhydrazine with trimethylamine dehydrogenase and with free flavins. *J. Biol. Chem. 254*, 2684–2688.
5. Kim, J. M., Hoegy, S. E., and Mariano, P. S. (1995) Flavin chemical-models for monoamine-oxidase inactivation by cyclopropylamines, alpha-silylamines, and hydrazines. *J. Am. Chem. Soc. 117*, 100–105.
6. Kenney, W. C., Nagy, J., Salach, J. I., and Singer, T. P. (1979) Structure of the Phenylhydrazine Adduct of Monoamine Oxidase, in *Monoamine Oxidase: Structure, Function and Altered Functions* (Singer, T. P., Von Korff, R. W., and Murphy, D., Eds.), pp 25−37, Academic Press, New York.
7. Demontellano, P. R. O., Augusto, O., Viola, F., and Kunze, K. L. (1983) Carbon radicals in the metabolism of alkyl hydrazines. *J. Biol. Chem. 258*, 8623–8629.
8. Fitzpatrick, P. F., and Villafranca, J. J. (1986) The mechanism of inactivation of dopamine beta-hydroxylase by hydrazines. *J. Biol. Chem. 261*, 4510–4518.
9. Newton-Vinson, P., Hubalek, F., and Edmondson, D. E. (2000) High-level expression of human liver monoamine oxidase B in *Pichia pastoris*. *Protein Expression Purif. 20*, 334–345.
10. Li, M., Hubalek, F., Newton-Vinson, P., and Edmondson, D. E. (2002) High-level expression of human liver monoamine oxidase A in *Pichia pastoris*: comparison with the enzyme expressed in Saccharomyces cerevisiae. *Protein Expression Purif. 24*, 152–162.
11. Binda, C., Newton-Vinson, P., Hubalek, F., Edmondson, D. E., and Mattevi, A. (2002) Structure of human monoamine oxidase B, a drug target for the treatment of neurological disorders. *Nat. Struct. Biol. 9*, 22–26.
12. De Colibus, L., Li, M., Binda, C., Lustig, A., Edmondson, D. E., and Mattevi, A. (2005) Three-dimensional structure of human monoamine oxidase A (MAO A): Relation to the structures of rat MAO A and human MAO B. *Proc. Natl. Acad. Sci. U.S.A. 102*, 12684–12689.
13. Silverman, R. B., Hoffman, S. J., and Catus, W. B. (1980) A Mechanism for mitochondrial monoamine-oxidase catalyzed amine oxidation. *J. Am. Chem. Soc. 102*, 7126–7128.
14. Kay, C. W. M., El Mkami, H., Molla, G., Pollegioni, L., and Ramsay, R. R. (2007) Characterization of the covalently bound anionic flavin radical in monoamine oxidase a by electron paramagnetic resonance. *J. Am. Chem. Soc. 129*, 16091–16097.
15. Ralph, E. C., Hirschi, J. S., Anderson, M. A., Cleland, W. W., Singleton, D. A., and Fitzpatrick, P. F. (2007) Insights into the mechanism of flavoprotein-catalyzed amine oxidation from nitrogen isotope effects on the reaction of N-methyltryptophan oxidase. *Biochemistry 46*, 7655–7664.
16. Miller, J. R., and Edmondson, D. E. (1999) Structure-activity relationships in the oxidation of para-substituted benzylamine analogues by recombinant human liver monoamine oxidase A. *Biochemistry 38*, 13670–13683.
17. Walker, M. C., and Edmondson, D. E. (1994) Structure-activity relationships in the oxidation of benzylamine analogues by bovine liver mitochondrial monoamine oxidase B. *Biochemistry 33*, 7088–7098.
18. Franot, C., Mabic, S., and Castagnoli, N., Jr (1998) Chemical model studies on the monoamine oxidase-B catalyzed oxidation of 4-substituted 1-cyclopropyl-1,2,3,6-tetrahydropyridines. *Bioorg. Med. Chem. 6*, 283–291.
19. Weyler, W., and Salach, J. I. (1985) Purification and properties of mitochondrial monoamine oxidase type A from human placenta. *J. Biol. Chem. 260*, 13199–13207.
20. Mayhew, S. G. (1999) Potentiometric Measurement of Oxidation-Reduction Potentials, in *Flavoprotein Protocols* (Chapman, S. K., and A., R. G., Eds.), pp 49−59, Humana Press, Totowa, NJ.
21. Binda, C., Li, M., Hubalek, F., Restelli, N., Edmondson, D. E., and Mattevi, A. (2003) Insights into the mode of inhibition of human mitochondrial monoamine oxidase B from high-resolution crystal structures. *Proc. Natl. Acad. Sci. U.S.A. 100*, 9750–9755.
22. Leslie, A. G. W. (1999) Integration of macromolecular diffraction data. *Acta Crystallogr., Sect. D 55*, 1696–1702.
23. Bailey, S. (1994) The Ccp4 Suite - Programs for Protein Crystallography. *Acta Crystallogr., Sect. D 50*, 760–763.
24. Murshudov, G. N., Vagin, A. A., and Dodson, E. J. (1997) Refinement of macromolecular structures by the maximum-likelihood method. *Acta Crystallogr. D Biol. Crystallogr. 53*, 240–255.
25. Morris, R. J., Perrakis, A., and Lamzin, V. S. (2002) ARP/wARP's model-building algorithms. I. The main chain. *Acta Crystallogr., Sect. D 58*, 968–975.
26. Emsley, P., and Cowtan, K. (2004) Coot: model-building tools for molecular graphics. *Acta Crystallogr., Sect. D 60*, 2126–2132.

27. Esnouf, R. M. (1999) Further additions to MolScript version 1.4, including reading and contouring of electron-density maps. *Acta Crystallogr., Sect. D 55*, 938–940.
28. Merritt, E. A., and Bacon, D. J. (1997) Raster3D: Photorealistic molecular graphics. *Macromol. Crystallogr., Pt B 277*, 505–524.
29. Yu, P. H., and Tipton, K. F. (1989) Deuterium-isotope effect of phenelzine on the inhibition of rat-liver mitochondrial monoamine-oxidase activity. *Biochem. Pharmacol. 38*, 4245–4251.
30. Kitz, R., and Wilson, I. B. (1962) Esters of methanesulfonic acid as irreversible inhibitors of acetylcholinesterase. *J. Biol. Chem. 237*, 3245–3250.
31. Hubalek, F., Pohl, J., and Edmondson, D. E. (2003) Structural comparison of human monoamine oxidases A and B: mass spectrometry monitoring of cysteine reactivities. *J. Biol. Chem. 278*, 28612–28618.
32. Binda, C., Mattevi, A., and Edmondson, D. E. (2002) Structure-function relationships in flavoenzyme-dependent amine oxidations: a comparison of polyamine oxidase and monoamine oxidase. *J. Biol. Chem. 277*, 23973–23976.
33. Li, M., Binda, C., Mattevi, A., and Edmondson, D. E. (2006) Functional role of the "aromatic cage" in human monoamine oxidase B: Structures and catalytic properties of Tyr435 mutant proteins. *Biochemistry 45*, 4775–4784.
34. Hubalek, F., Binda, C., Khalil, A., Li, M., Mattevi, A., Castagnoli, N., and Edmondson, D. E. (2005) Demonstration of isoleucine 199 as a structural determinant for the selective inhibition of human monoamine oxidase B by specific reversible inhibitors. *J. Biol. Chem. 280*, 15761–15766.
35. Zhao, Y. Y., Bordwell, F. G., Cheng, J. P., and Wang, D. F. (1997) Equilibrium acidities and homolytic bond dissociation energies (BDEs) of the acidic H-N bonds in hydrazines and hydrazides. *J. Am. Chem. Soc. 119*, 9125–9129.
36. Walker, W. H., Hemmeric., P., and Massey, V. (1967) Reductive Photoalkylation of flavin nucleus and flavin catalyzed photodecarboxylation of phenyl acetate. Studies in flavin series 0.15. *Helv. Chim. Acta 50* 2269–2279.
37. Huang, P. K. C., and Kosower, E. M. (1967) Properties of phenyldiimide. *J. Am. Chem. Soc. 89*, 3910–3911.
38. Kosower, E. M. (1971) Monosubstituted diazenes (diimides) - surprising intermediates. *Acc. Chem. Res. 4*, 193–198.
39. Huang, Y. Q., Guler, L., Heidbrink, J., and Kenttamaa, H. (2005) Reactions of charged phenyl radicals with aliphatic amino acids in the gas phase. *J. Am. Chem. Soc. 127*, 3973–3978.
40. Han, J. Y., Swarts, J. C., and Sykes, A. G. (1996) Kinetic studies on the hydrazine and phenylhydrazine reductions of the *Escherichia coli* R2 subunit of ribonucleotide reductase. *Inorg. Chem. 35*, 4629–4634.
41. Mure, M., Brown, D. E., Saysell, C., Rogers, M. S., Wilmot, C. M., Kurtis, C. R., McPherson, M. J., Phillips, S. E. V., Knowles, P. F., and Dooley, D. M. (2005) Role of the interactions between the active site base and the substrate Schiff base in amine oxidase catalysis. Evidence from structural and spectroscopic studies of the 2-hydrazinopyridine adduct of *Escherichia coli* amine oxidase. *Biochemistry 44*, 1568–1582.
42. Newton-Vinson, P., and Edmondson, D. E. (1999) High-Level Expression, Structural, Kinetic, and Redox Characterization of Recombinant Human Liver Monoamine Oxidase B, in *Flavins and Flavoproteins* (Ghisla, S., Kroneck, P., Macheroux, P., and H., S., Eds.), pp 431−434, Agency for Scientific Publications, Berlin.
43. Edwards, J. O., and Pearson, R. G. (1962) Factors determining nucleophilic reactivities. *J. Am. Chem. Soc. 84*, 16–24.
44. Edmondson, D. E., Binda, C., and Mattevi, A. (2007) Structural insights into the mechanism of amine oxidation by monoamine oxidases A and B. *Arch. Biochem. Biophys. 464*, 269–276.

BI8002814